

# A new constraint on cosmological variability of the proton-to-electron mass ratio<sup>\*</sup>

S. A. Levshakov,<sup>1†</sup> M. Dessauges-Zavadsky,<sup>2‡</sup> S. D’Odorico,<sup>2</sup> and P. Molaro<sup>3</sup>

<sup>1</sup> *Division of Theoretical Astrophysics, National Astronomical Observatory, Tokyo 181-8588, Japan*

<sup>2</sup> *European Southern Observatory, Karl-Schwarzschild-Str. 2, D-85748 Garching bei München, Germany*

<sup>3</sup> *Osservatorio Astronomico di Trieste, Via G.B. Tiepolo 11, I-34131 Trieste, Italy*

Accepted . Received ; in original form

## ABSTRACT

Exotic cosmologies predict variability of the fundamental physical constants over the cosmic time. Using the VLT/UVES high resolution spectra of the quasar Q0347–3819 and unblended electronic-vibrational-rotational lines of the H<sub>2</sub> molecule identified at  $z_{\text{abs}} = 3.025$  we test possible changes in the proton-to-electron mass ratio  $\mu_0 = m_p/m_e$  over the period of  $\sim 11$  Gyr. We obtained a new constraint on the time-averaged variation rate of  $\mu_0$  of  $|\dot{\mu}/\mu_0| < 5 \times 10^{-15} \text{ yr}^{-1}$  ( $1\sigma$  c.l.). The estimated  $1\sigma$  uncertainty interval of the  $|\Delta\mu/\mu_0|$  ratio of about 0.004% implies that since the time when the H<sub>2</sub> spectrum was formed at  $z_{\text{abs}} = 3.025$ ,  $\mu_0$  has not changed by more than a few thousands of a percent.

**Key words:** cosmology: observations – elementary particles – quasars: absorption lines – quasars: individual: Q0347–3819

## 1 INTRODUCTION

Kaluza-Klein (KK) type models (Super-symmetric Grand Unification Theory, Super string models, etc.) unify gravity with other fundamental forces. These models predict variations of the fundamental physical constants over the cosmological evolution (for a review, see, e.g., Okun’ 1991). Variations of the coupling constants of strong and electroweak interactions would affect the masses of the elementary particles in a way which depends on the adopted scenario for the expanding universe. The model parameters of these theories can be constrained by observations. One possibility to test values of the physical constants at different cosmological epochs is to study high resolution spectra of extragalactic objects (Saviedoff 1956).

Such analysis has been recently carried out by a number of authors (see, e.g., Varshalovich, Potekhin & Ivanchik 2000, and references cited therein), and a possible variation of the fine-structure constant,  $\alpha_0 = e^2/\hbar c$ , at a level of  $\Delta\alpha/\alpha_0 = (-0.72 \pm 0.18) \times 10^{-5}$  was announced by Webb et al. (2001) who analyzed fine-splitting lines in quasar spectra.

The first restriction on the variability of the proton-to-

electron mass ratio<sup>4</sup>,  $\mu_0 = m_p/m_e$ , stemming from quasar spectra  $|\Delta\mu/\mu_0| < 0.13$  ( $1\sigma$  c.l.) was obtained by Pagel (1977) who compared the observational wavelengths of H I and metals as previously proposed by Thompson (1975). However, the derived upper limit on  $\mu_0$  depends on the assumption that all elements have the same fractional ionization ratios and trace the same volume elements along the respective line of sight. This assumption may not be true in general especially for QSO absorbers where complex absorption-line profiles are observed at high spectral resolution.

The proton-to-electron mass ratio can be estimated more accurately from high redshift molecular hydrogen systems. With some modifications, such measurements were performed for the  $z_{\text{abs}} = 2.811$  H<sub>2</sub> system from the spectrum of PKS 0528–250 by Foltz, Chaffe & Black (1988), Varshalovich & Levshakov (1993), Cowie & Songaila (1995), and by Potekhin et al. (1998) who set the most stringent limit of  $|\Delta\mu/\mu_0| < 1.8 \times 10^{-4}$  ( $1\sigma$  c.l.).

In this paper, we present a new upper limit on the variation rate of the proton-to-electron mass ratio obtained from the analysis of a new H<sub>2</sub> system found at  $z_{\text{abs}} = 3.025$  toward the quasar Q0347–3819.

<sup>\*</sup> Based on public data released from UVES Commissioning at the VLT Kueyen telescope, ESO, Paranal, Chile

<sup>†</sup> On leave from the Ioffe Physico-Technical Institute, Russian Academy of Sciences, St. Petersburg

<sup>‡</sup> Affiliated to Observatoire de Genève, CH–1290 Sauverny, Switzerland

<sup>4</sup> The present value of the proton-to-electron mass ratio is  $\mu_0 = 1836.1526670$  (Mohr & Taylor 2000).

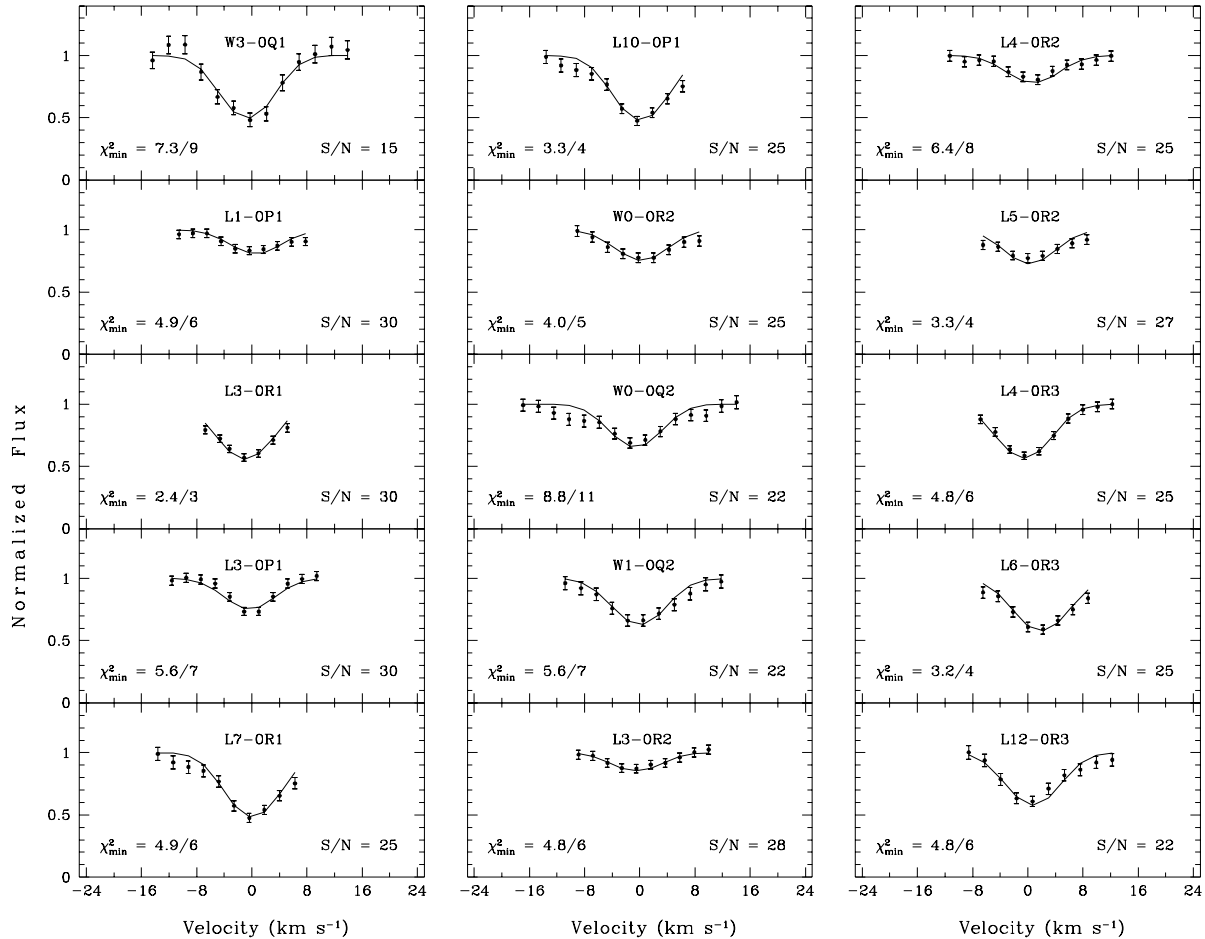


**Figure 1.** H<sub>2</sub> absorption features associated with the  $z_{\text{abs}} = 3.025$  damped Ly $\alpha$  system toward Q0347–3819 (renormalized intensities shown by dots with  $1\sigma$  error bars were calculated for the mean values of the local continuum deviations  $\Delta C/C$  listed in Table 1). The zero radial velocity is fixed at  $z_{\text{H}_2} = 3.024895$ . Smooth curves are the synthetic H<sub>2</sub> profiles found by the least-squares procedure as described in the text. The best ( $\chi^2/\text{degree of freedom}$ ) values and the mean  $S/N$  per resolution element are shown in the corresponding panels.

## 2 OBSERVATIONS

High resolution spectra of the quasar Q0347–3819 were obtained during UVES commissioning at the VLT 8.2m ESO telescope and are described in detail by D’Odorico, Dessauges-Zavadsky & Molaro (2001) and Levshakov et al. (2002, LDDM hereinafter). The spectrum resolution is  $\text{FWHM} \simeq 7.0 \text{ km s}^{-1}$  and  $5.7 \text{ km s}^{-1}$  in the UV and near-IR ranges, respectively. The signal-to-noise ratio per resolution element in the UV range is  $S/N \sim 10 - 40$ .

We identified more than 80 H<sub>2</sub> molecular lines in a damped Ly $\alpha$  system (DLA hereinafter)<sup>5</sup> at  $z_{\text{abs}} = 3.025$  toward Q0347–3819 (LDDM). Some of them are not suitable for further analysis due to H I Ly $\alpha$  forest contamination. However, we selected 15 unblended H<sub>2</sub> lines (shown in

Fig. 1) which provide the most accurate line center measurements to set an upper limit on possible changes of  $\mu_0$ .

We would like to emphasize that our analysis of the  $z_{\text{abs}} = 3.025$  DLA has shown that all the H<sub>2</sub> line profiles can be adequately described with a unique value of  $z_{\text{H}_2} = 3.024855 \pm 0.000005$ <sup>6</sup> which implies that no assumption on the variability of  $\mu_0$  is needed or *statistically justified*. Observations show that the ratio  $\Delta\mu/\mu_0 \equiv (\mu_z - \mu_0)/\mu_0$  is zero. The analysis presented below has the objective to estimate at what accuracy  $\Delta\mu/\mu_0 = 0$ .

## 3 DATA ANALYSIS AND RESULTS

For measurements of the absorption line centers in QSO spectra, there are three principal sources of statistical errors

<sup>5</sup> The damped Ly $\alpha$  systems are believed to originate in the intervening galaxies or proto-galaxies located at cosmological distances (e.g. Wolfe et al. 1995).

<sup>6</sup> Based on the H<sub>2</sub> laboratory wavelengths given in Abgrall & Roueff (1989).

**Table 1.** H<sub>2</sub> lines at  $z_{\text{abs}} = 3.025$  toward Q0347–3819 and sensitivity coefficients  $\mathcal{K}$ .

$J$ (1)	Line (2)	$\lambda_0^a$ , Å (3)	$\Delta C/C^b$ , % (4)	$\lambda_{\text{obs}}$ , Å (5)	$z$ (6)	$\mathcal{K}$ (7)
1	W3-0Q	947.4218±0.0005	0.9 ± 0.2	3813.2653 ± 0.0041	3.024887(5) <sup>d</sup>	0.0217427(8)
	L1-0P	1094.0522±0.0051 <sup>c</sup>	0.8 ± 0.1	4403.4575 ± 0.0077	3.02491(2)	−0.0023282(1)
	L3-0R	1063.4603±0.0001 <sup>c</sup>	0.8 ± 0.1	4280.3051 ± 0.0030	3.024885(3)	0.0112526(4)
	L3-0P	1064.6056±0.0005	0.9 ± 0.2	4284.9249 ± 0.0033	3.024894(4)	0.0102682(4)
	L7-0R	1013.4412±0.0020	0.8 ± 0.1	4078.9785 ± 0.0025	3.024898(9)	0.03050(1)
	L10-0P	982.8340±0.0006	0.8 ± 0.1	3955.8049 ± 0.0051	3.024896(6)	0.04054(6)
2	W0-0R	1009.0233±0.0007	0.8 ± 0.1	4061.2194 ± 0.0061	3.024901(7)	−0.0050567(7)
	W0-0Q	1010.9380±0.0001	0.8 ± 0.1	4068.9088 ± 0.0053	3.024885(6)	−0.0068461(2)
	W1-0Q	987.9744±0.0020	0.9 ± 0.1	3976.4943 ± 0.0049	3.02490(1)	0.0039207(2)
	L3-0R	1064.9935±0.0009	1.0 ± 0.2	4286.4755 ± 0.0098	3.02488(1)	0.0097740(5)
	L4-0R	1051.4981±0.0004 <sup>c</sup>	0.8 ± 0.1	4232.1793 ± 0.0085	3.024904(8)	0.015220(1)
	L5-0R	1038.6855±0.0032	0.8 ± 0.1	4180.6048 ± 0.0070	3.02490(1)	0.020209(3)
3	L4-0R	1053.9770±0.0011	0.8 ± 0.1	4242.1419 ± 0.0028	3.024890(5)	0.012837(2)
	L6-0R	1028.9832±0.0016	0.8 ± 0.1	4141.5758 ± 0.0031	3.024921(7)	0.022332(7)
	L12-0R	967.6752±0.0021	0.8 ± 0.1	3894.7974 ± 0.0039	3.02490(1)	0.0440(2)

Notes: <sup>a</sup> listed values are from Abgrall et al. (1993a, 1993b); <sup>b</sup> the local continuum deviation with 1 $\sigma$  error; <sup>c</sup> the error is estimated from the comparison between the data in Abgrall & Roueff (1989) and Abgrall et al. (1993a, 1993b); <sup>d</sup> 1 $\sigma$  standard deviations are shown in parenthesis (last digits after a decimal point), e.g. 3.024887(5) means  $3.024887 \pm 0.000005$ .

caused both by the data reduction procedure and by statistical fluctuations in the recorded counts. First, all echelle data must be rebinned to constant wavelength bins in order to combine different spectra and hence to increase the signal-to-noise ratio. Such resampling changes statistical properties of the noise and introduces correlations between the data point values. The correlation coefficient of about +0.8 was estimated by LDDM for the UVES data in question. This means that the classical  $\chi^2$  test is *no longer applicable* to the rebinned spectra, because the measurements are not independent. The second error, usually important for lines observed in the Ly $\alpha$  forest, arises from the uncertainty of the overall continuum level and its shape in the vicinities of individual spectral features. The third error is connected with the finite number of photons counted. The individual intensity points within the interval of integration can fluctuate producing distortions in the line shape.

There are, of course, other sources of errors in the measurements of the precise wavelengths  $\lambda_{\text{obs}}$  of the observed H<sub>2</sub> lines. The values of  $\lambda_{\text{obs}}$  may be affected by errors in the wavelength calibration and by the thermal shifts. The observed wavelengths are not significantly affected by errors in the correction of the wavelength scale to the heliocentric and vacuum values. Typically, these errors do not exceed a few m s<sup>−1</sup> (e.g. Edlén 1953). The quasar spectrum is, however, constantly shifted with temperature by 0.37 pixel/K. Given the approximate pixel size (0.02 Å) at 4000 Å, we can expect the shift of at most 0.3 km s<sup>−1</sup> in case the Th calibration spectrum was taken a few hours after the science exposures and the difference in temperature was 0.5 K. The thermal shift should be more or less constant for all lines, so it affects only the assumed redshift. The values of  $\lambda_{\text{obs}}$  are mainly affected by errors in the wavelength calibration. We found that the rms of this systematic error over the total range covered by the blue spectrum is  $\sigma_{\text{sys}} = \pm 0.0016$  Å. This corresponds at 4000 Å to 0.12 km s<sup>−1</sup>.

The continuum placement in the UV portion of the

Q0347–3819 spectrum was determined by using ‘continuum windows’ in the Ly $\alpha$  forest which were fitted by a low order polynomial. The accuracy  $\delta_c$  of the local continuum (which may deviate from the common continuum in the Ly $\alpha$  forest region) was estimated during the fitting procedure described below.

For a given H<sub>2</sub> line, the number of pixels involved in the analysis corresponds to the number of points in the line profile shown in Fig. 1. To measure the line centers we used a method that matches the observed profiles with the synthesized ones to estimate the set of model parameters. Our previous analysis of the line profiles of different elements identified in the  $z_{\text{abs}} = 3.025$  H<sub>2</sub>-bearing cloud has shown that both low ions and H<sub>2</sub> have the same simple velocity structure of the main component – a narrow symmetrical core with a common broadening parameter  $b_{\text{H}_2} = 2.80 \pm 0.45$  km s<sup>−1</sup> (LDDM). Thus in our present study we also used a simple one-component model with four free parameters: the center, the width, the intensity of the absorption line and the local continuum displacement  $\delta_c = \Delta C/C$  (this technique was successfully used in the study of metal lines in the Ly $\alpha$  forest by Molaro et al. 2001). The set of initial parameters then was adjusted until a satisfactory fit could be achieved. The objective function was augmented with the penalty function in the form [cf. Eqs. (13) and (14) in LDDM]:

$$\psi = \left( \frac{b - b_{\text{H}_2}}{\sigma_{b_{\text{H}_2}}} \right)^2, \quad (1)$$

where  $b_{\text{H}_2} = 2.80$  km s<sup>−1</sup> and  $\sigma_{b_{\text{H}_2}} = 0.45$  km s<sup>−1</sup>.

To evaluate statistical errors, Monte Carlo analysis was performed in the same way as described in Appendix A in LDDM. The results of these calculations are presented in columns (4) and (5) of Table 1. It is seen that for the selected H<sub>2</sub> lines  $\delta_c \simeq 1\%$ . This means that the H<sub>2</sub> lines involved in

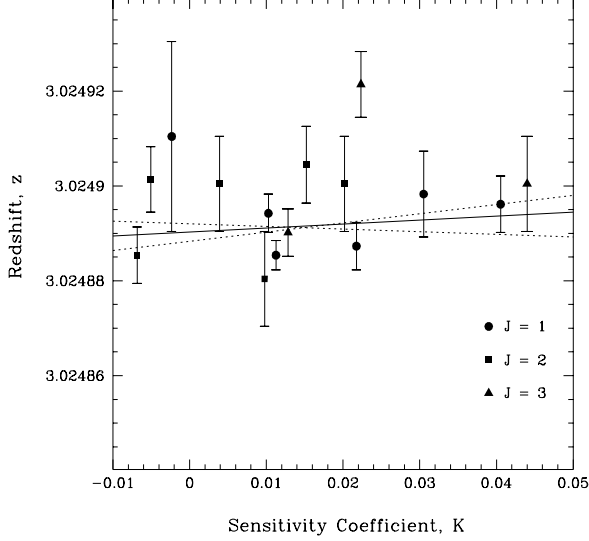


**Figure 2.** Relation between the redshift values  $z_i$  calculated for individual  $H_2$  features shown in Fig. 1 and their sensitivity coefficients  $\mathcal{K}_i$ . The solid line is the linear regression:  $z_i = \bar{z} + \kappa(\mathcal{K}_i - \bar{\mathcal{K}})$  with  $\kappa = (1 + \bar{z})\Delta\mu/\mu_0$ . The dotted lines representing the  $1\sigma$  deviations from the slope  $\kappa$  of the best linear regression demonstrate that  $\Delta\mu/\mu_0 \equiv 0$  at the level  $\sim 3 \times 10^{-5}$ .

the analysis are not significantly disturbed by the Ly $\alpha$  forest absorption.

In this approach the central wavelengths  $\lambda_{\text{obs}}$  can be measured with an accuracy exceeded the average pixel size. As expected, the weaker absorption features have lower accuracy compared with the stronger lines. The corresponding redshifts for individual  $H_2$  lines are shown in column (6) with the  $1\sigma$  uncertainties including  $\sigma_{\text{syst}}$ . In these calculations we used the  $H_2$  laboratory wavelengths  $\lambda_0$  from Abgrall et al. (1993a, 1993b) which show slightly different  $\lambda_0$  values as compared with their previous publication (Abgrall & Roueff 1989). Therefore, as a consequence the new values of  $z_{H_2}$  discussed below are shifted with respect to those presented in LDDM.

With the obtained  $z$  values and their standard deviations we are able to constrain possible changes of  $\mu_0$ . Indeed, if the ratio  $\Delta\mu/\mu_0 \equiv (\mu_z - \mu_0)/\mu_0$  is not zero, then for any two  $H_2$  lines with rest frame wavelengths  $\lambda_{i,0}$  and  $\lambda_{j,0}$  the ratio

$$\frac{\lambda_{i,z}/\lambda_{j,z}}{\lambda_{i,0}/\lambda_{j,0}} \simeq 1 + (\mathcal{K}_i - \mathcal{K}_j) \Delta\mu/\mu_0 \quad (2)$$

would deviate from unity, where  $\lambda_{i,z}$  and  $\lambda_{j,z}$  are the corresponding line centers measured in a quasar spectrum.

In equation (2), the so-called sensitivity coefficients  $\mathcal{K}$  determine the sensitivity of  $H_2$  wavelengths to the variation of the proton-to-electron mass ratio. These coefficients have been calculated by Varshalovich & Levshakov (1993) and in a different manner by Varshalovich & Potekhin (1995). Both methods give results in good agreement. The most recent version of the procedure to calculate  $\mathcal{K}$  and  $\Delta\mu/\mu_0$  from QSO spectra is described in detail by Potekhin et al. (1998). Following this procedure we calculated the sensitivity coefficients which are listed in column (7) of Table 1. The accuracy of the  $\mathcal{K}$  values was also estimated from coefficients

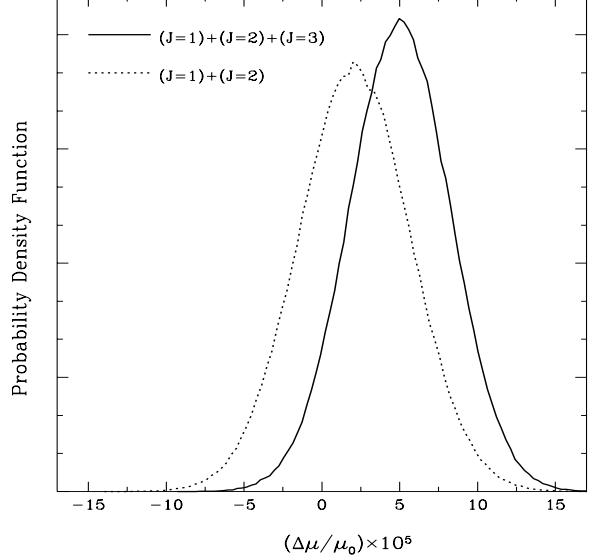


**Figure 3.** Monte Carlo simulations of the probability density functions (p.d.f.) of  $\Delta\mu/\mu_0$  for two samples: (i) the  $H_2$  lines arising from the low rotational levels with  $J = 1, 2, 3$  (the solid curve), and (ii) the  $H_2$  lines arising from the low rotational levels with  $J = 1, 2$  (the dashed curve). The difference between p.d.f. is caused by gradual shift in the radial velocity as  $J$  increases.

$Y_{mn}$  (listed in Table 1 in Potekhin et al.) using the method of error propagation ( $Y_{mn}$  values were considered to be accurate to  $k$  decimal places and their rounding errors were set to  $0.5 \times 10^{-k}$ ). It should be noted that although transitions between the excited states of the  $H_2$  molecule have higher wavelength-to-mass sensitivity coefficients, their accuracy is much lower as compared with the low- $J$  transitions. In linear approximation

$$z_i = \bar{z} + \kappa(\mathcal{K}_i - \bar{\mathcal{K}}), \quad (3)$$

where  $\kappa = (1 + \bar{z})\Delta\mu/\mu_0$  with  $\bar{z}$  and  $\bar{\mathcal{K}}$  being the mean redshift and the mean sensitivity coefficient, respectively.

The linear regression in the form (3) was firstly calculated for the complete sample of the  $H_2$  lines (Table 1) where transitions from the  $J = 1, 2$  and 3 levels are combined. The obtained result  $(\Delta\mu/\mu_0)_{J=1+2+3} = (5.0 \pm 3.2) \times 10^{-5}$  (which is consistent with the value independently found by Ivanchik et al. 2002) shows a “possible variation” of  $\mu_0$  at the  $1.6\sigma$  level. However, if we consider  $H_2$  transitions from individual  $J$  levels, then the weighted mean redshifts reveal a *gradual shift in the radial velocity* for features arising from progressively higher rotational levels:  $z_{H_2}^{J=1} = 3.024890(2)$ ,  $z_{H_2}^{J=2} = 3.024895(3)$ , and  $z_{H_2}^{J=3} = 3.024904(4)^7$ . The  $H_2$  lines with changing profiles and small velocity shifts as  $J$  increases were also observed in our Galaxy in the direction of  $\zeta$  Ori A by Jenkins & Peimbert (1997) who suggested that these  $H_2$  lines are formed in *different* zones of a postshock gas.

Albeit the  $z_{H_2}^{J=1}$  and  $z_{H_2}^{J=2}$  values are consistent within  $1\sigma$  intervals, the difference between  $z_{H_2}^{J=1}$  and  $z_{H_2}^{J=3}$  is essential and equals  $1.0 \pm 0.3 \text{ km s}^{-1}$ . If we now exclude from the regression analysis levels with  $J = 3$ , then  $(\Delta\mu/\mu_0)_{J=1+2} =$

<sup>7</sup> The numbers shown in parenthesis are the  $1\sigma$  standard deviations in last digits after a decimal point.

$(2.1 \pm 3.6) \times 10^{-5}$ . (The use of samples with H<sub>2</sub> lines arising from the same rotational levels would be more reasonable to estimate  $\Delta\mu/\mu_0$ , but in our case the sample size is rather small and we have to combine the  $J = 1$  and  $J = 2$  levels to increase accuracy). This linear regression is shown by the solid line in Fig. 2 while two dashed lines correspond to the  $1\sigma$  deviations of the slope parameter  $\kappa$ .

We also calculated the probability density functions of  $\Delta\mu/\mu_0$  for two samples of the H<sub>2</sub> lines (with  $J = 1, 2, 3$ , and  $J = 1, 2$ ) using statistical Monte Carlo simulations which suggest that the errors  $\sigma_z$  and  $\sigma_K$  are normally distributed around the mean values of  $z$  and  $K$  with the dispersions equal to their probable errors listed in Table 1. The result is presented in Fig. 3. It is clearly seen that small changes in the radial velocity with increasing  $J$  cause the difference between these two probability density functions and thus may mimic a shift in  $\Delta\mu/\mu_0$ .

From these calculations we find  $|\Delta\mu/\mu_0| < 5.7 \times 10^{-5}$  ( $1\sigma$ ) which is about three times stronger as compared with the value estimated by Potekhin et al. (1998).

Both constraints on the variation of the  $m_p/m_e$  ratio are in good agreement with the limit on the variability of the product of the fine-structure constant, nuclear  $g$  factor of the proton and the masses of the electron and proton  $\Delta\ln(\alpha^2 g_p m_e/m_p) = (1.2 \pm 1.8) \times 10^{-4}$  which was set by de Bruyn, O'Dea & Baum (1996) from the measurements of the redshifts of the H I 21 cm line and the optical resonance absorption lines observed at  $z_{\text{abs}} = 3.38$  in the DLA toward Q0201+113. The same order of magnitude restrictions to  $\Delta\ln(\alpha^2 g_p m_e/m_p)$  were found from other DLAs detected at  $z_{\text{abs}} = 0.524$  (Q0235+164), 0.692 (3C286), 1.944 (Q1157+014), and 2.038 (Q0458-020) (see Table 4 in de Bruyn et al. 1996), and even stronger limit of  $(0.7 \pm 1.1) \times 10^{-5}$  at  $z_{\text{abs}} = 1.776$  (Q1331+170) was set by Cowie & Songaila (1995). Comparison of H I 21 cm and molecular absorption (CO, <sup>13</sup>CO, C<sup>18</sup>O, CS, HCO<sup>+</sup>, and HCN) also yields very tight constraints on the ratio  $|\Delta(\alpha^2 g_p)/(\alpha^2 g_p)_0| \lesssim 0.7 \times 10^{-5}$  at  $z_{\text{abs}} = 0.2467$  and 0.6847 toward Q1413+135 and Q0218+357, respectively (Murphy et al. 2001).

In our calculations the  $1\sigma$  confidence interval to  $\Delta\mu/\mu_0$  was set as

$$-1.5 \times 10^{-5} < \Delta\mu/\mu_0 < 5.7 \times 10^{-5}.$$

For a cosmological model with  $\Omega_M = 0.3$ ,  $\Omega_\Lambda = 0.7$ , and  $H_0 = 72 \text{ km s}^{-1} \text{ Mpc}^{-1}$ , the look-back time for  $z_{\text{abs}} = 3.025$  is 11.2 Gyr [see, e.g., equation (16) in Carroll, Press, & Turner 1992]. This leads to the restriction

$$|\dot{\mu}/\mu_0| < 5 \times 10^{-15} \text{ yr}^{-1}$$

on the variation rate of  $\mu_0$ .

## 4 CONCLUSIONS

We have obtained a new constraint on the variation rate of the proton-to-electron mass ratio of  $\Delta\mu/\mu_0 = (2.1 \pm 3.6) \times 10^{-5}$  at  $z_{\text{abs}} = 3.025$  toward Q0347-3819 ( $\Delta t \simeq 11 \text{ Gyr}$ ). The accuracy is a factor of 3 higher as compared with the measurements in another H<sub>2</sub>-bearing cloud at  $z_{\text{abs}} = 2.811$  toward Q0528-250 (Potekhin et al. 1998). Both measurements show no statistically significant changes of  $\mu_0$  on space and time coordinates.

Since the functional dependence of the masses of proton and electron on the fine-structure constant is unknown, we are not able to compare directly our result with changes in  $\alpha$  at the level of  $\sim 0.7 \times 10^{-5}$  found by Webb et al. (2001).

## ACKNOWLEDGMENTS

S.A.L. gratefully acknowledges the hospitality of the National Astronomical Observatory of Japan, where these results have been obtained. The authors thank A. V. Ivanchik and D. A. Varshalovich for useful discussion, and our anonymous referee for many helpful suggestions. The work of S.A.L. is supported in part by the RFBR grant No. 00-02-16007.

## REFERENCES

- Abgrall H., Roueff E., 1989, A&AS, 79, 313
- Abgrall H., Roueff E., Launay F., Roncin J.-Y., Subtil J.-L., 1993a, A&ASS, 101, 273
- Abgrall H., Roueff E., Launay F., Roncin J.-Y., Subtil J.-L., 1993b, A&ASS, 101, 323
- Carroll S.M., Press W.H., Turner E.L., 1992, ARA&A, 30, 499
- Cowie L.L., Songaila A., 1995, ApJ, 453, 596
- de Bruyn A.G., O'Dea C.P., Baum S.A., 1996, A&A, 305, 450
- D'Odorico S., Dessauges-Zavadsky M., Molaro, P., 2001, A&A, 368, L1
- Edlén B., 1953, J. Opt. Soc. Am., 43, 339
- Foltz C.B., Chaffee F.H., Black J.H., 1988, ApJ, 324, 267
- Jenkins E.B., Peimbert A., 1997, ApJ, 477, 265
- Levshakov S.A., Dessauges-Zavadsky M., D'Odorico S., Molaro P., 2002, ApJ, 565, 696 [LDDM]
- Mohr P.J., Taylor B.N., 2000, Rev. Mod. Phys. 72, 351
- Molaro P., Levshakov S.A., D'Odorico S., Bonifacio P., Centurión M., 2001, ApJ, 549, 90
- Murphy M. T. et al. 2001, MNRAS, 327, 1244
- Okun' L.B., 1991, Usp. Fiz. Nauk, 161, 177
- Pagel B., 1977, MNRAS, 179, 81P
- Potekhin A.Y. et al., 1998, ApJ, 505, 523
- Savedoff M.P., 1956, Nature, 178, 3511
- Thompson R., 1975, Astron. Lett., 16, 3
- Varshalovich D.A., Levshakov S.A., 1993, JETP Lett., 58, 237
- Varshalovich D.A., Potekhin A.Y., 1995, Space Sci. Rev., 74, 259
- Varshalovich D.A., Potekhin A.Y., Ivanchik A.V., 2000, in X-Ray and Inner-Shell Processes, eds. R.W. Dunford et al. (American Institute of Physics, Melville, New York), p. 503
- Webb J.K. et al., 2001, PhRvL, 87, 1301
- Wolfe A.M., Lanzetta K.M., Foltz C.B., Chaffee F.H., 1995, ApJ, 454, 698